ALGERIAN JOURNAL OF ENGINEERING AND TECHNOLOGY

Algerian Journal of Engineering and Technology
ISSN: 2716-9227 (Print)
EISSN: 2716-9278 (Online)
DOI:
Mernache et al / vol. 10, n°2 - 2025

Original Article Open Access

Influence of hydrogen reduction temperature in a fluidized bed on AUC derived UO_2 powder properties

Mernache Fatah[a]*, Benaouicha Farid[a], Ladjouzi Samia[a], Amrane Amina[a], Melhani Yasmine[a], Aoudia Nacera[a], Korichi Smain[b], Serrai Salim[a], Messai Lakhdar[a], Grine Mohamed[a]

[a] *Draria Nuclear Research Center (CRND), BP 43, Draria, Algiers, Algeria.; f-mernache@crnd.dz*
[b] *Atomic Energy Commission (COMENA), 2, boulevard Frantz Fanon, BP 399, 16000 Algiers, Algeria.*
* *Corresponding author.* E-mail address: f-mernache@crnd.dz
Article history: Received 01 September 2025, Revised 29 September 2025, Accepted 05 October 2025

ABSTRACT

The production of uranium dioxide (UO_2) powders by calcination–reduction of ammonium uranyl carbonate (AUC, $(NH_4)_4UO_2(CO_3)_3$) is an important step in the UO_2 fuel pellet fabrication process. The nature and quality of the resulting UO_2 depend closely on the initial characteristics of AUC as well as on the applied thermal treatment conditions. The UO_2 powders obtained must meet specific requirements, particularly those related to specific surface area (4.5–7 m²/g) and particle size distribution. The objective of this work is to analyze the effect of the hydrogen reduction temperature on the properties of AUC-derived UO_2 powders using a fluidized-bed furnace. In this study, the reduction temperature of AUC was varied from 400 to 550 °C, and the resulting UO_2 powders were characterized. The O/U ratio, specific surface area, and particle size distribution of the UO_2 powders were determined respectively by spectrophotometry, nitrogen adsorption–desorption (BET method), and laser granulometry. During tests on stabilization of the AUC powder bed, it was observed that the minimum fluidization flow rate ranged between 20 and 30 L/min. Within this range, a proportional relationship was observed between the pressure drop and the fluidization velocity. Beyond 30 L/min, the fluidized bed became stable. As the reduction temperature increased from 400 to 550 °C, the specific surface area decreased from 10.2 to about 7 m²/g (±0.2 m²/g). However, the particle size distribution of the UO_2 powders varied only slightly with temperature. A reduction temperature of 550 °C under hydrogen in a fluidized bed was selected as the optimal condition for the conversion of AUC into UO_2 powder exhibiting good sintering properties for nuclear fuel pellet production (7 m²/g).

Keywords: AUC powder; fluidized-bed furnace; calcination–reduction; UO_2 powder; specific surface area.

Graphical abstract

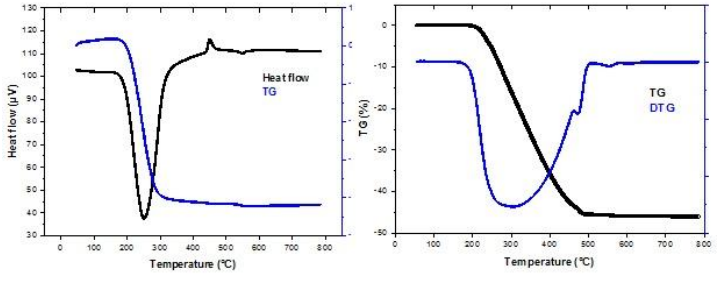

DTA/TG (a) and TG/DTG (b) curves of AUC decomposition in nitrogen atmosphere at 10 °C/min heating rate

Recommended Citation
Mernache F, Benaouicha F, Ladjouzi S, Amrane A, Melhani Y, Aoudia N, Korichi S, Serrai S, Messai L, Grine M. Influence of hydrogen reduction temperature in a fluidized bed on AUC derived UO_2 powder properties. *Alger. J. Eng. Technol.* 2025, 10(2): 53-60

1. Introduction

The compound ammonium uranyl carbonate (AUC), with the chemical formula (NH4)UO(CO3)3, was first obtained by Bazelius in 1824 during the preparation of uranyl carbonate [1,2]. It is an intermediate product in the nuclear fuel fabrication process, where it undergoes a conversion step into UO_2 powder [3–6]. However, the pressing and sintering behavior of the resulting UO_2 powder is closely related to the characteristics of the starting AUC powder and to the AUC-to-UO_2 conversion process.

In this conversion process, the most critical operation affecting the properties of the uranium dioxide powder is the reduction of AUC-derived oxides to UO2. It has been reported [5] that the drying step of AUC prior to calcination has no significant effect on the characteristics of the resulting UO_2 powder.

AUC begins to decompose through an endothermic reaction at approximately 125 ± 5 °C [4, 6]. The decomposition products include amorphous or crystalline UO_3, NH_4, CO_2, and H_2O [1–4, 8, 9]. However, the maximum temperature of the endothermic DTA peak shifts toward higher values when the atmosphere used contains one of the gases released during the decomposition [7]. The final product obtained is either U3O8 or UO2, depending on the atmosphere used.

The final product obtained in air, helium, Argon or nitrogen is U3O8, whereas in hydrogen it is UO_2 [8, 10, 11]. Hälldahl and Sørensen [8] proposed the formation of several intermediate amorphous hydrated phases of the type UO_3 (H2O)x (with x ranging from 2.0 down to 0.25), which dehydrate progressively. During the reduction sequence, U3O8, is assumed to form as an intermediate between UO_3 and UO_2 in the presence of hydrogen [4,9,10,12].

Numerous studies reported in the literature focus on the transformation of AUC into UO_2 using DTA-TG, DSC–TG or TG analyses [13-19], whereas, to the best of the authors' knowledge, relatively few works investigate the elaboration of UO2 derived from AUC or ADU in a fluidized-bed reactor [20,21].

The purpose of this research is to investigate various aspects of the fluidized-bed treatment of AUC powder. This paper examines the conversion of AUC-derived oxides as a function of temperature.

2. Materials and Methods

The AUC powder used in this study was of high purity, containing 45.70 ± 0.5 wt% uranium. Before use, it was dried in an oven at 50 °C for 22 hours. According to the product's technical data sheet, its chemical composition is as follows: UO_2 – 51.85% (U = 45.70%), CO_3 – 34.38%, NH_4 – 13.77%, and H2O – <0.5%.

The thermal analyses were carried out using a simultaneous differential thermal and thermogravimetric analyzer (DTA-TG) and a thermogravimetric analyzer (TG), both manufactured by SETARAM, model TG 96. For more detailed on AUC, see ref. 11.

Preliminary investigations were conducted using a SETARAM thermogravimetric analyzer (TG96). Further experiments were then carried out in a fluidized-bed furnace (multipurpose reactor, maximum operating temperature 700 °C) coupled with a hydrogen–nitrogen–steam gas supply system. We investigated using simultaneous DTA-TG and TG analyses the influence of two atmospheres (N2, and an Ar–H_2 mixture containing 10% H_2 by volume) on the thermal decomposition of AUC. It should be noted that using thermogravimetric (TG) curves alone provides better measurement accuracy compared to simultaneous DTA-TG analysis. This improvement is attributed to the fact that the amount of AUC used in the TG experiments was increased by a factor of 50.

To characterize the powder properties, the specific surface area was measured by the BET method using an ASAP surface area analyzer (ASAP 20210, Micromeritics). The average particle size and particle size distribution were determined using a laser diffraction particle size analyzer (Analysette 22, Fritsch). The O/U ratio of the intermediate phases and the resulting uranium oxide powders were analyzed by UV–Vis spectrophotometry (GBC UV/VIS 918 PHERA).

A fluidized-bed furnace capable of operating up to 700 °C under different atmospheres (N2 and/or H2) was used for the preparation of sinterable UO_2powders. The main components of the furnace include the auxiliary systems (power supply, process gases, heating, and temperature control), the diffuser plate, the reactor, and the loading/unloading system.

3. Results and Discussion

The specific surface area of the AUC powder, determined by nitrogen adsorption using the BET method on a Micromeritics ASAP 2000 analyzer, is 0.16 m²/g. The average particle size of the AUC powder is 44.4 µm. The results of D10, D50 and D90 ares:

D(v,0.5)	D(v,0.1)	D(v,0.9)
27.63 µm	**14.84 µm**	**50.83 µm**

3.1. Treatment of AUC in TG/DTA

3.1.1. Treatment of AUC under N2

The decomposition of AUC begins at approximately 118 °C under an industrial nitrogen atmosphere (Figure 1). According to this figure, several transformation peaks can be observed:

- A first peak between 194 °C and 313 °C (Δm = 41.34 %)
- A second peak between 440 °C and 468 °C (Δm = 0.3 %)
- A third peak between 533 °C and 562 °C (Δm = 0.43 %).

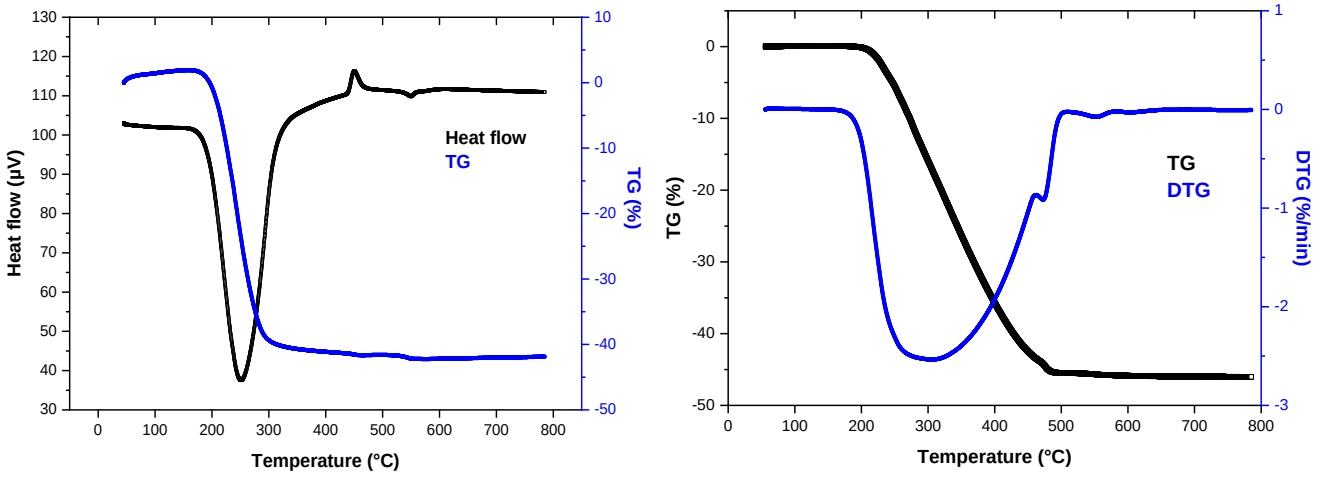

Fig 1. DTA/TG (a) and TG/DTG (b) curves of AUC decomposition in nitrogen atmosphere at 10 °C/min heating rate

The total weight loss determined from the TG curve (Figure 1) is 1.84 g, corresponding to 46.05%.

Analysis of the TG/DTG curves (Figure 1b) reveals that AUC decomposition in nitrogen begins at ~160 °C and continues up to ~350 °C. The formation of anhydrous UO_3 occurs at around 400 °C and is associated with the exothermic peak observed on the DTG curve at 252°C." A full transformation of AUC into U3O8 is associated with a mass loss of approximately 45.2% [13]. The total weight loss determined from the TG curve (Figure 1) is 1.84 g, corresponding to 46.03%. This value is in very good agreement with the theoretical mass loss associated with the stoichiometric conversion of AUC to U_3O_8 (≈46.3%).

3.1.2. Treatment of AUC under an argon–hydrogen (90–10%) mixture

The decomposition of AUC (Figure 2) begins at approximately 150 °C under an atmosphere consisting of an argon–hydrogen mixture with respective volume proportions of 90% Ar and 10% H_2. According to figure 2, several transformation peaks are observed:

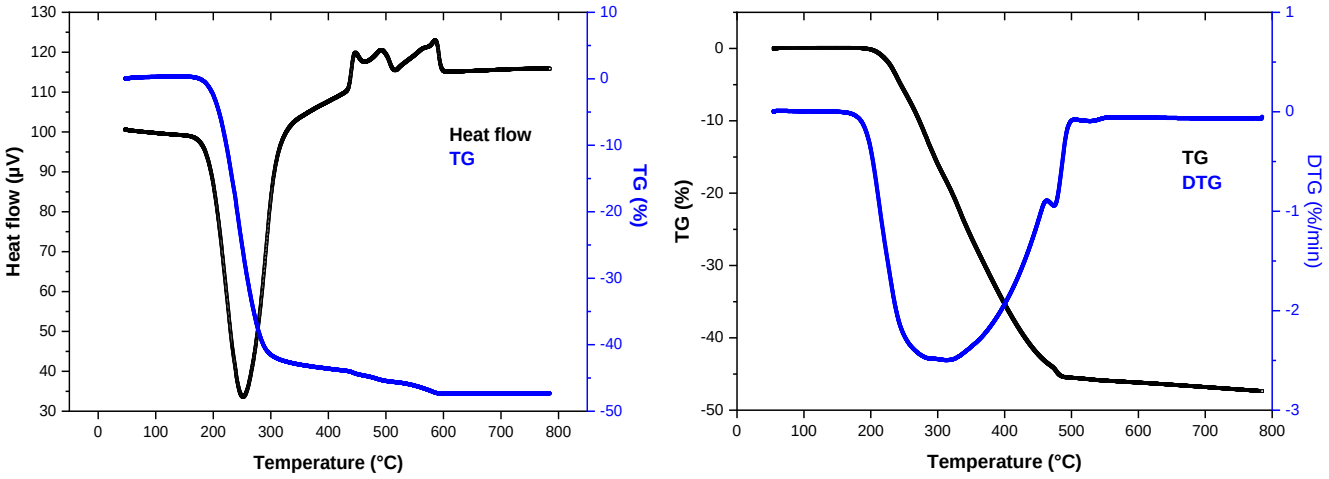

Fig 2. DTA (a) and TG (b) curves of AUC decomposition 90%Ar–10%H_2 atmosphere at 10 °C/min heating rate

- A first peak between 191 °C and 314 °C (Δm = 43.93 %): (formation of amorphous UO_3 phase)
- A second peak between 437 °C and 461 °C, (Δm = 0.99 %) (UO_3 cristallization)
- A third peak between 503 °C and 554 °C, (Δm = 2.01 %) (formation of U_3O_8 phase)
- A fourth peak between 575 °C and 594 °C, (Δm = 0.61 %) (formation of UO_2 phase)

AUC begins to decompose at approximately 190 ± 5 °C in all experiments, according to Equation (1) below. Based on the TG, DTA-TG curves, and in comparison with stoichiometric calculations, the intermediate product formed after decomposition is identified as $UO_3(H_2O)_x$, with **x** ranging from 0 to 1.5.

$$(NH_4)_4UO_2(CO_3)_3\ (s) \longrightarrow UO_3(H_2O)_x\ (s) + 4NH_3\ (g) + 3CO_2\ (g) + (2\text{-}x)H_2O\ (g) \qquad (1)$$

For X=0 :

$$(NH_4)_4UO_2(CO_3)_3\ (s) \longrightarrow UO_3\ (s) + 4NH_3\ (g) + 3CO_2\ (g) + 2H_2O\ (g) \qquad (2)$$

Equation (1) is approximate, since it has been reported [3, 6] that the amorphous UO_3 matrix contains not only UO_3 and H_2O but also traces of carbon and nitrogen. However, according to L. Hälldahl *et al.* [8], these traces of carbon and nitrogen were not detected.

The decomposition reaction is endothermic, and the corresponding temperature peaks vary depending on the atmosphere used. From the DTA-TG curves obtained under the different atmospheres studied, the onset temperatures of decomposition and those corresponding to the maxima of the endothermic peaks were determined. These values are presented in figure 1 and 2 and summarized in Table 1.

Table 1. The mass loss data and temperature range for the decomposition of AUC at different atmospheres (first pic, 10°C/min- 800°C)

Atmosphere	**T_i (°C)**	**T_f (°C)**	**T_{pick} (°C)**	**Weight loss (%)**
N_2	194	313	252	41.34
Ar-H_2 (90-10)	191	314	252	43.93

Table 2 below summarizes the mass losses values of the final products (in percentage) with respect to stoichiometric AUC. These values were obtained using two different methods: The first method, based on the analysis of the curves

shown in Figures 1 and 2, provides higher accuracy. The second method, used as a verification, consists in determining the mass loss by weighing, i.e., from the difference between the initial weight of the AUC and that of the final product. This method is less accurate than the first one.

Under an Ar–H_2 atmosphere, the final product formed is UO_2, whereas under N_2 atmosphere, the final product obtained is U_3O_8.The influence of the atmosphere (inert or reducing) on AUC decomposition is described by the mass loss data and temperature range (Table 2). Under an inert N_2 atmosphere, the weight loss reached ~46%, while under a reducing H_2 atmosphere it was ~47.4 %.

Table 2. Weight losses of the final products obtained with respect to stoichiometric AUC (10°C/min-800°C)

Atmosphere	Total weight loss (TG) (%)	Total weight loss (by weighing) (%)	O/U ratio of the final products	Final product
N_2	46.03	46.25	2.64	U_3O_8
Ar-H_2 (90-10)	47.37	48.25	2.05	$UO_{2.05}$

The determination of the O/U ratio by spectrophotometry under N_2 leads to the formation of a product close to U_3O_8 (O/U ratio = 2.64). With the reducing H_2, we confirmed the formation of a slightly hyperstoichiometric oxide $UO_{2.05}$ (O/U ration= 2.05).

3.2. Treatment of AUC in Fluidized-bed furnace

The fluidized-bed treatment was carried out using a multipurpose reactor operating under controlled gas flow conditions. The reactor allows precise regulation of temperature, gas composition, and flow rate to ensure uniform fluidization of the AUC powder. This setup enables efficient heat and mass transfer between the reacting gas and the solid particles, thereby promoting homogeneous decomposition and reduction processes.

The characteristic curves of the distribution plate (diffuser plate) for the calcination–hydrogen reduction treatment of AUC at 400, 450, 500 and 550 (Figure 3) were determined by injecting nitrogen at flow rates ranging from 20 to 80 L/min.

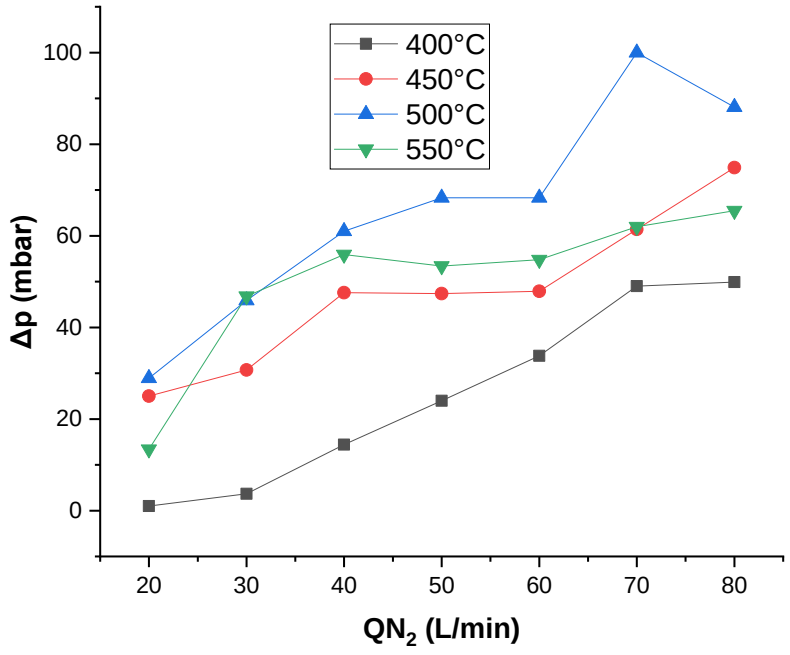

Fig 3. Determination of the distribution plate curve of AUC in the fluidized-bed furnace: a) 400, b) 450, c) 500 and d) 550 °C.

The curves shown in Figure 3 illustrate the relationship between the pressure drop (Δp) and the nitrogen flow velocity through the beds of uranium powder particles. Based on Figures 3a, 3b and 3c (450, 500 and 550 °C), the minimum fluidization velocity is found to be between 20 and 40 L/min, indicating a proportional relationship between the pressure

drop and the fluidization velocity. Beyond 40 L/min, the fluidized bed becomes stable until 60 L/min. Figure 4 illustrates the variation of the three treatment temperatures (T_{up}, $T_1/_2$, and T_{low}) as a function of AUC decomposition time.

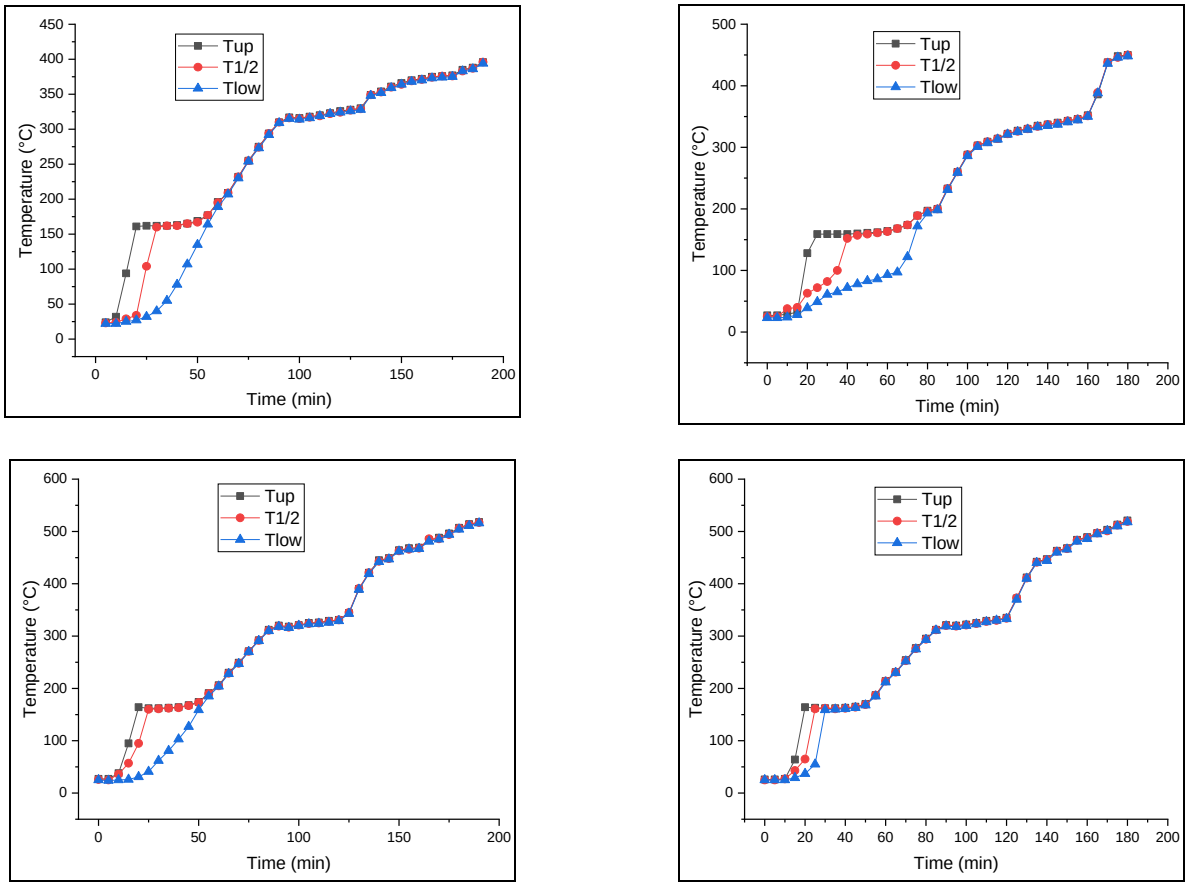

Fig 2. Effect of the final calcination temperature (onset reduction temperature) in the fluidized-bed furnace on the decomposition of AUC at: a) 400, b) 450, c) 500 and d) 550 C.

During the calcination (decomposition) of AUC (Fig. 4), deviations in the recorded temperature values (Tup, $T_{1/2}$, and T_{low}) are observed up to one hour of treatment (< about 200 °C), which indicates the occurrence of powder compaction. This phenomenon was observed for all treatments, with a time shift depending on the experimental conditions.

The reduction temperature effect on the surface area of UO_2 powders produced from AUC in a fluidized-bed furnace is shown in figure 5. It has been shown [22] that several physical characteristics strongly influence the sinterability of UO_2 powders, including the surface area, the O/U ratio, the flowability, and the green density.

As the reduction temperature increased from 400 to 550 °C, the surface area decreased from 10.2 to about 7 m^2/g (±0.2 m^2/g). Choi *et al.* [23] reported that, although the calcination and reduction of AUC to UO_2 do not noticeably modify the particle morphology, they significantly influence physical properties. A significant amount of porosity develops during the conversion of AUC to UO_2. This porosity is directly reflected in the green pellet and establishes the initial microstructural state that governs sintering behavior, thereby influencing the final density of the pellet [7, 11].

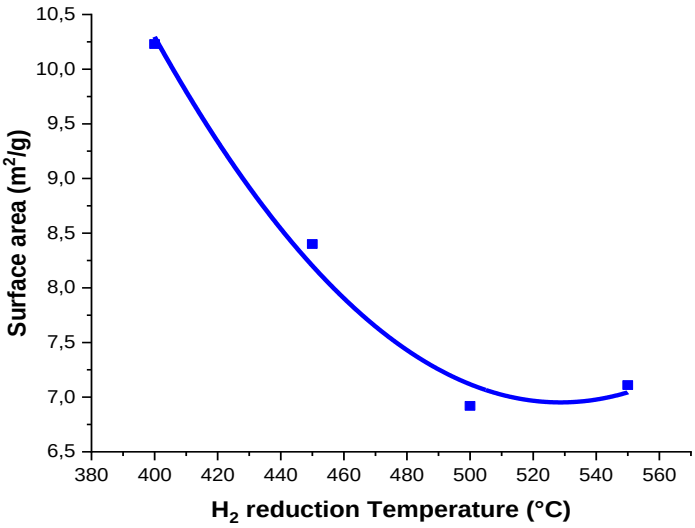

Figure 5: Influence of the hydrogen reduction temperature on the specific surface area of UO_2 powders produced from AUC in a fluidized-bed furnace (holding time at the reduction temperature: 60 min)

The increase in the specific surface area of UO_2 compared to the initial AUC precursor results from the thermal effect associated with its decomposition, which induces the formation of porosity up to approximately 350 °C. Thus, the specific surface area increases during the dehydration and decomposition steps due to the opening of internal porosity caused by stress-induced cracking within the particles. These internal stresses arise from the nucleation and growth of phases that exhibit molar volumes differing from that of the parent solid.

During the reduction step of the calcined AUC powder at temperatures higher than 400 °C, the surface area decreases due to crystallite growth [23], sintering, and the progressive closure of porosity [11]. Upon stabilization in air, the O/U stoichiometry of the UO_2 powders produced at 400–550 °C is found to be in the range 2.11–2.17, in good agreement with the results reported in the literature [5]. In general, UO_2 powders exhibit O/U ratios between 2.06 and 2.17; however, compositions below 2.06 do not result in improved sintered densities [6].

4. Conclusion

In this study, the Transformation of AUC to UO2 was performed in DTA/TG, TG and fluidized-bed furnace. The specific surface area of UO_2 powders decreases from 10.2 to ~7 m²/g between 400 and 550 °C, with the PSD changing little, and 550 °C in H_2 is identified as the optimal condition to obtain UO_2 powder suitable for sintering into fuel pellets. The identified hydrodynamic parameters (Umf 20–30 L/min, stability >30 L/min) provide operating guidelines to ensure uniform treatment in a fluidized bed at pilot or industrial scale.

During the decomposition of the AUC at different final temperatures in fluidized-bed furnace (400, 450, 500 and 550 °C), deviations in the temperature values (Tup, T1/2, and Tlow) were observed within the first hour (< about 200 °C), suggesting the occurrence of powder compaction. This behavior was consistently observed across all treatments, with a temporal shift depending on the experimental conditions. An increase in the reduction temperature from 400 to 550 °C resulted in a decrease in the specific surface area from 10.2 to approximately 7 m²/g (± 0.2 m²/g).

A reduction temperature of 550 °C under hydrogen in a fluidized bed was identified as the optimal condition for converting AUC into UO_2 powder with suitable sintering properties for nuclear fuel pellet fabrication (7 m²/g).

Ethical Statement

This study does not contain any studies with human or animal subjects performed by any of the authors.

Conflict of Interest

The authors declare that they have no conflict of interest.

References

1. Kim EH, Park JJ, Chang JH, Choi CS, Kim SD. Thermal decomposition kinetics of ammonium uranyl carbonate. *J Nucl Mater*. 1994;209:294–300. https://doi.org/10.1016/0022-3115(94)90266-6
2. Bachmann HG, Seibold K, Dokuzoguz HZ, Müller HM. X-ray powder diffraction and some thermodynamic data for $(NH_4)_4[UO_2(CO_3)_3]$. *J Inorg Nucl Chem*. 1975;37:735–737.
3. Hälldahl L. Study of the composition of the amorphous phase formed during decomposition of ammonium uranyl carbonate in various atmospheres. *Thermochim Acta*. 1985;95:389–394. https://doi.org/10.1016/0040-6031(85)85300-4
4. Hälldahl L. In situ studies of the decomposition of ammonium uranyl carbonate in an electron microscope. *J Nucl Mater*. 1984;126:170–176. https://doi.org/10.1016/0022-3115(84)90087-4
5. Kondal Rao N, et al. Technological aspects of UO_2 fuels: Characterisation and quality control – Indian experience. *J Nucl Mater*. 1979;81:171–176. https://doi.org/10.1016/0022-3115(79)90075-8
6. Hälldahl L, Nygren M. Thermal analysis studies of the reactions occurring during the decomposition of ammonium uranyl carbonate in different atmospheres. *J Nucl Mater*. 1986;138:99–106. https://doi.org/10.1016/0022-3115(86)90260-6
7. Marajofsky A, Pérez L, Celora J. On the dependence of characteristics of powders on the AUC process parameter. *J Nucl Mater*. 1991;178:143–151. https://doi.org/10.1016/0022-3115(91)90379-L
8. Hälldahl L, Sørensen T. Thermal analysis of the decomposition of ammonium uranyl carbonate (AUC) in different atmospheres. *Thermochim Acta*. 1979;29:253–259. https://doi.org/10.1016/0040-6031(79)87084-7
9. Hälldahl L, Nygren M. TG, DSC, X-ray and electron diffraction studies of intermediate phases in the reduction of ammonium uranyl carbonate to UO_2. *Thermochim Acta*. 1984;72:213–218.
10. Korichi S, Aoudia N, Benlmadjet H, Kaci S, Ousmaal N. Kinetic studies of isothermal decomposition of $(NH_4)_4UO_2(CO_3)_3$ to uranium oxide. *Prog React Kinet Mech*. 2020;45. https://doi.org/10.1177/1468678319888629
11. Korichi S, Mernache F, Benaouicha F, Aoudia N, Amrane A, Hadji S. Thermal behavior and kinetic modeling of $(NH_4)_4UO_2(CO_3)_3$ decomposition under non-isothermal conditions. *J Radioanal Nucl Chem*. 2017;314:923–934. https://doi.org/10.1007/s10967-017-5444-2
12. Le Page AH, Fane AG. The kinetics of hydrogen reduction of UO_3 and U_3O_8 derived from ammonium diuranate. *J Inorg Nucl Chem*. 1974;36:87–94. https://doi.org/10.1016/0022-1902(74)80663-9
13. Girgis BS, Rofail NH. Decomposition–reduction stages of ammonium uranyl carbonates under different atmospheres. *Thermochim Acta*. 1992;196:105–115. https://doi.org/10.1016/0040-6031(92)85010-S
14. Pijolat M, Brun C, Valdivieso F, Soustelle M. Reduction of uranium oxide U_3O_8 to UO_2 by hydrogen. *Solid State Ionics*. 1997;101–103:931–935. https://doi.org/10.1016/S0167-2738(01)00730-5
15. Tel H, Eral M. Investigation of production conditions and powder properties of AUC. *J Nucl Mater*. 1996;231:165–169. https://doi.org/10.1016/0022-3115(96)00354-6
16. Baran V, Vošček V. Spontaneous isothermal decomposition of the uranyl carbonate complex $(NH_4)_4[UO_2(CO_3)_3]$ at room temperature. Part II: Infrared spectroscopy and X-ray analysis. *Thermochim Acta*. 1987;122(2):261–276. https://doi.org/10.1016/0040-6031(87)87047-8
17. Bing-Guo L, Jin-Hui P, Srinivasakannan C, Li-Bo Z, Jin-Ming H, Sheng-Hui G, Dong-Cheng K. Preparation of U_3O_8 by calcination from ammonium uranyl carbonate in microwave fields: Process optimization. *Ann Nucl Energy*. 2015;85:879–884.
18. Qingre G, Shifang K. Study of AUC thermal decomposition kinetics in nitrogen by a non-isothermal method. *Thermochim Acta*. 1987;116:71–77. https://doi.org/10.1016/0040-6031(87)88166-2
19. Ki BH, Lee YB, Prelas MA, Ghosh TK. Thermal and X-ray diffraction analysis during the decomposition of ammonium uranyl nitrate. *J Radioanal Nucl Chem*. 2012;292:1075–1083. https://doi.org/10.1007/s10967-011-1579-8
20. Gomes RP, Riella HG, Instituto de Pesquisas Energéticas e Nucleares (IPEN). Development of a reduction process of ammonium uranyl carbonate to uranium dioxide in a fluidized bed. In: *Proceedings of the II CGEN – General Congress on Nuclear Energy*; 1988; Rio de Janeiro, Brazil.
21. Cho WD, Han MH, Bronson MC, Zundelevich Y. Processing of uranium oxide powders in a fluidized-bed reactor. I. Experimental. *J Nucl Mater*. 2002;305:106–111. https://doi.org/10.1016/S0022-3115(02)01135-2
22. Patro JB, Sridharan AK, Katiyar NPS, Sampath M, Rajendran R, Sinha KK, Kondal Rao N. UO_2 fuels – Qualitative approach for characterization. *J Nucl Mater*. 1982;106:81–86. https://doi.org/10.1016/0022-3115(82)90335-X
23. Choi CS, Park JH, Kim EH, Shin HS, Chang IS. The influence of AUC powder characteristics on UO_2 pellets. *J Nucl Mater*. 1988;153:148–155. https://doi.org/10.1016/0022-3115(88)90206-1